# Interaction between sine-Gordon breathers

P. G. Kevrekidis, A. Saxena, and A. R. Bishop
*Theoretical Division, Los Alamos National Laboratory, Los Alamos, New Mexico 87545*

(Received 7 April 2001; published 25 July 2001)

Using the exact breather lattice solution of the sine-Gordon equation, we obtain the asymptotic interaction between two breathers. We identify the exponential dependence of the interaction on the breather separation as well as its power-law dependence on the breather frequency. Numerical simulation of the breather lattice demonstrates its instability. However, stabilization of such structures is found to be feasible through ac driving and damping. Finally, other limits of the original periodic solution are traced, obtaining the leading-order terms in the interaction between ''pseudosphere'' solutions and kink-antikink pairs.

DOI: 10.1103/PhysRevE.64.026613 PACS number(s): 41.20.Jb, 63.20.Pw

The $1+1$ dimensional sine-Gordon equation ($u_{xx}-u_{tt}=\sin u$) appears in a wide variety of physical systems, including charge-density-wave materials, magnetic flux in Josephson lines, splay waves in membranes, Bloch-wall motion in magnetic crystals, and models of elementary particles, among others [1]. In the context of differential geometry, its solutions correspond to surfaces of constant negative curvature [2]. As part of the Ablowitz-Kaup-Newell-Segur hierarchy of integrable partial differential equations [3], this equation has an exact single soliton solution, a soliton-antisoliton solution, and a breather solution. In addition, it also has exact spatially periodic solutions such as a soliton lattice and a breather lattice [2]. A breather is a spatially localized, time periodic nonlinear mode. Breathers can directly affect electronic, optical, and transport properties of a material [4–6]. Specifically, they can enhance optical nonlinearities in polyenes and related low-dimensional electronic materials [4,5]. Therefore, in addition to its fundamental significance in nonlinear systems, it is important to understand the interaction between breathers.

There are several methods of obtaining the (asymptotic) interaction between solitons [7]. One of them is to use the soliton lattice (i.e., periodic wave train) solution and calculate its energy in the ''dilute'' limit [8], i.e., when the modulus of the elliptic function is close to unity. In this paper, our objective is to calculate the breather interaction analytically, using the exact breather lattice solution. In particular, we study the dependence of the interaction as a function of breather temporal period (or frequency) and spatial period. We then determine the stability of the configurations using the *exact* breather lattice and introducing perturbations only through the discretization of the spatial domain. In this way we find the configuration to be unstable. However, we are able to stabilize it in the more realistic setting (for physical applications) of damping and ac driving. The sine-Gordon breather interactions have been experimentally studied recently using inelastic neutron scattering [9]. Interactions between two breathers have also been analyzed in the context of the nonlinear coupled Klein-Gordon equations [10] and numerically studied for a coupled electron-vibron lattice system [6]. Our results may therefore be expected to be relevant also for other systems with soft nonlinearities, as well as for their envelope wave equations such as the nonlinear Schrödinger (NLS) equation. In the latter case, in fact, it is known that the interaction between such coherent structures decays exponentially with increasing separation and is attractive for ''pulses'' of the same parity, while repulsive for ones of opposite parity (see, e.g., [11] and references therein).

The periodic breather lattice solution of the sine-Gordon (SG) equation is given by [2]

$$u(x,t)=4\tan^{-1}[a\,\mathrm{sn}(bt,k^2)\,\mathrm{dn}(cx,1-m^2)], \tag{1}$$

where $\mathrm{sn}(x,k)$, $\mathrm{cn}(x,k)$ (below), and $\mathrm{dn}(x,m)$ are the Jacobi elliptic functions with modulus $k$ or $m$. A breather lattice solution for specific values of $k,m$ is depicted in Fig. 1. Note that with respect to the notation of Ref. [2], we use $x-y\to t$, $x+y\to x$ (in agreement with the standard notation for the SG equation). Here,

$$a=\sqrt{\frac{k}{m}},\quad b=\sqrt{\frac{m}{(m+k)(1+mk)}},$$
$$c=\sqrt{\frac{k}{(m+k)(1+mk)}}. \tag{2}$$

For the SG equation, the energy is given by

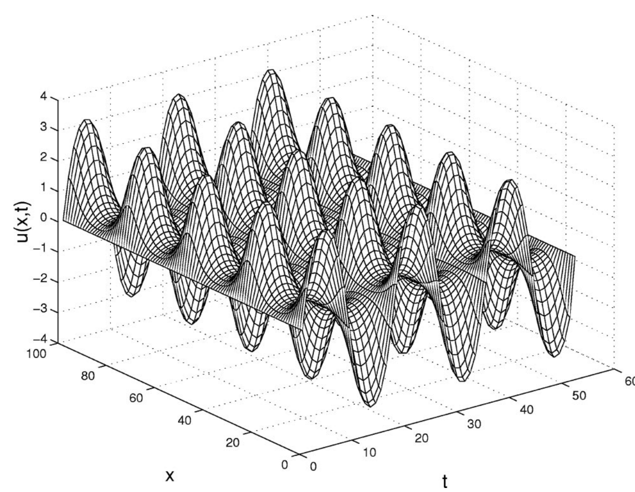


FIG. 1. Pictorial representation of the exact sine-Gordon breather lattice solution. Shown is a fraction of the field $u(x,t)$ containing exactly four breathers and demonstrating their propagation for a time interval equal to three times the period of each breather.

 ©2001 The American Physical Society

$$E=\int E_d dx=\int\left[\frac{u_x^2+u_t^2}{2}+(1-\cos u)\right]dx. \tag{3}$$

Substitution of Eq. (1) into Eq. (3) gives the spatial energy density

$$E_d=\frac{8km^2\mathrm{cn}^2(bt,k^2)\mathrm{dn}^2(cx,1-m^2)\mathrm{dn}^2(bt,k^2)+4k^2(1-m^2)^2\mathrm{cn}^2(cx,1-m^2)\mathrm{sn}^2(cx,1-m^2)\mathrm{sn}^2(bt,k^2)}{(c+m)(1+km)[m+k\mathrm{dn}^2(cx,1-m^2)\mathrm{sn}^2(bt,k^2)]^2}+\frac{(8k/m)\mathrm{dn}^2(cx,1-m^2)\mathrm{sn}^2(bt,k^2)}{[1+(k/m)\mathrm{dn}^2(cx,1-m^2)\mathrm{sn}^2(bt,k^2)]^2}. \tag{4}$$

Since the result of integration of Eq. (3) (over $x$) will be independent of $t$, we evaluate the expression (4) at $t=0$ first and then integrate. To be mathematically precise $E=E(t=0)=\lim_{t\to 0}E=\lim_{t\to 0}\int E_d dx=\int dx \lim_{t\to 0}E_d$. Then

$$E_d(t=0)=\frac{16k\mathrm{dn}^2(cx,1-m^2)}{(k+m)(1+km)}. \tag{5}$$

We now integrate Eq. (5) up to the spatial period $2K(1-m^2)/c$ to obtain

$$E=\int_0^{2K(1-m^2)/c}E_d dx=16\sqrt{\frac{k}{(k+m)(1+km)}}E(1-m^2), \tag{6}$$

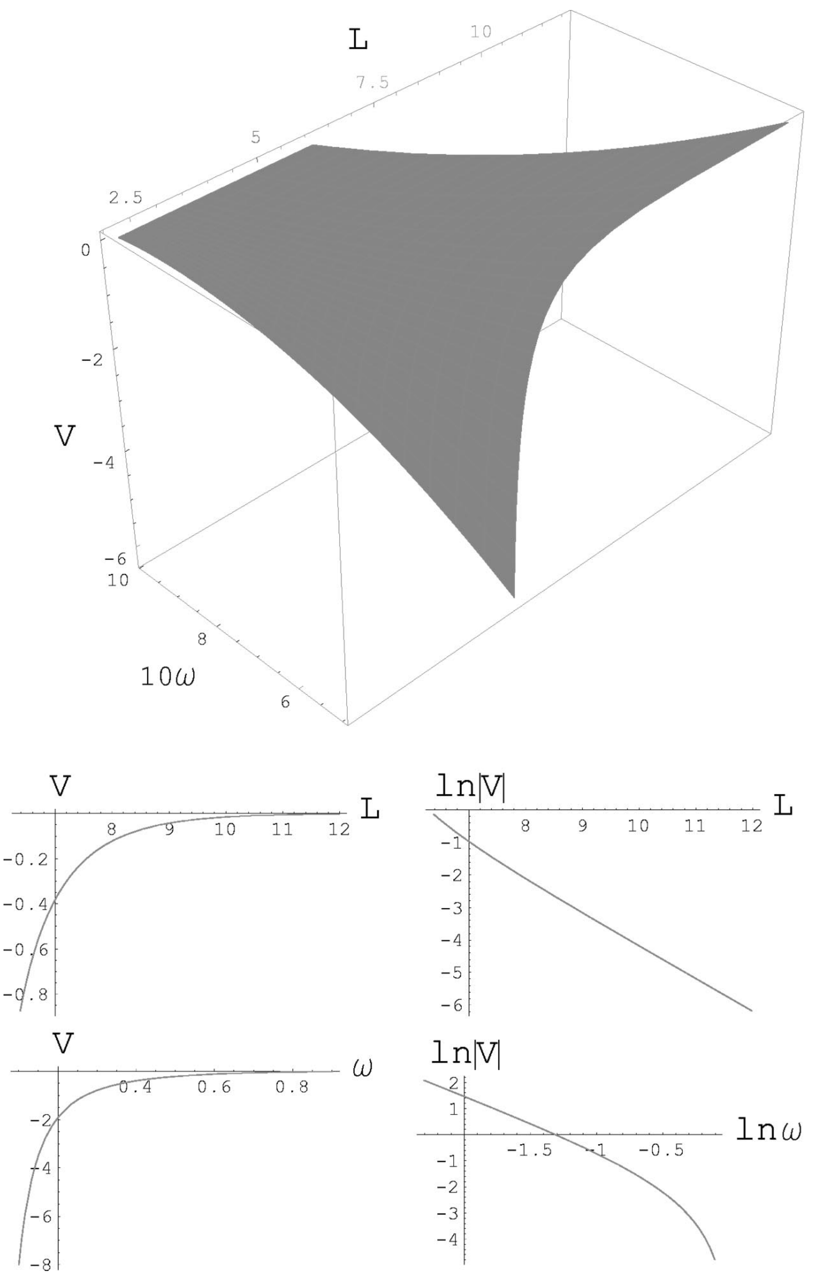


FIG. 2. The interaction energy $V$, defined in the text, is given for the breather lattice configuration as a function of the breather frequency $\omega$ and the breather separation $L$ in the 3D plot of the top panel. Instead of $\omega$, $10\omega$ has been used for clarity. Two-dimensional sections of the top panel are shown in the two pairs of the bottom panels. The first two show, in linear and log-linear plots, the dependence of $V$ on $L$ for fixed $\omega$, while the second pair demonstrates the dependence of $V$ on $\omega$ for fixed $L$ in linear and log-log plots (also see text).

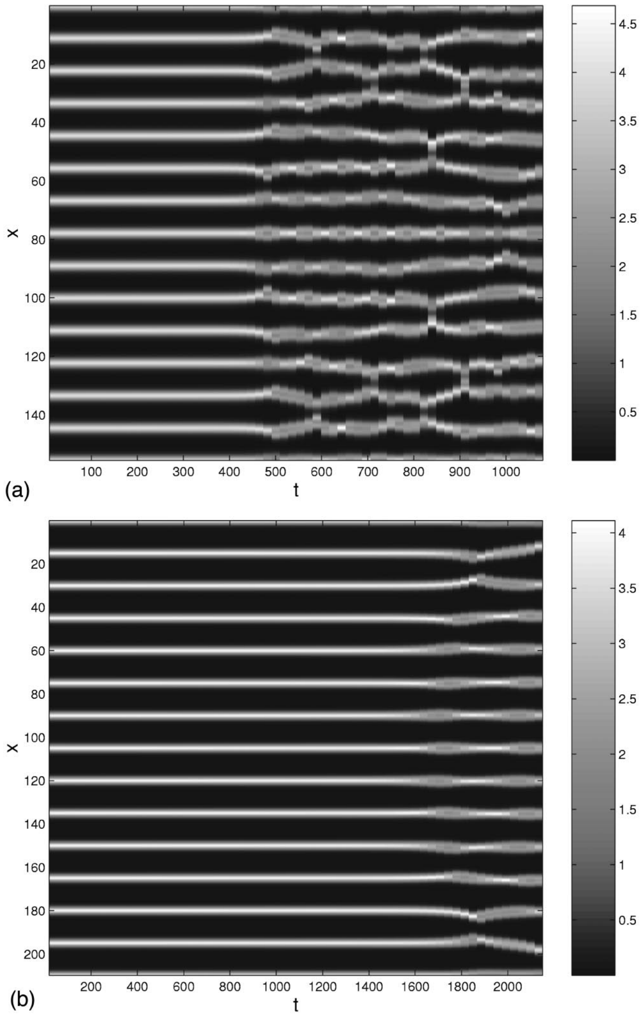


FIG. 3. A space time contour plot of the spatial energy density is shown for two different cases (corresponding to different breather separations) for both of which $\omega^2=0.5$. The top panel corresponds to $(k,m)=(0.08,0.08)$, while the bottom to $(k,m)=(0.02,0.02)$. In the latter case, the distance between the breathers is larger, and hence, it takes longer for the perturbation due to discreteness (of the originally symmetric and periodic configuration) to cause the breather interaction to destroy the unstable breather lattice configuration.

where $K(1-m^2)$ and $E(1-m^2)$ are the complete elliptic integrals of the first and second kind, respectively.

Equation (6) is an important result used below to obtain the asymptotic interaction between the two breathers. The breather lattice solution of Eq. (1) is depicted numerically in Fig. 1 for a typical set of parameters $(k,m)$. To calculate the breather-breather interaction, we take the limit $m,k\to 0$, with $k/m=(1-\omega^2)/\omega^2$, where $\omega$ is the breather frequency. Then Eq. (6) becomes

$$E=\left[16\sqrt{1-\omega^2}-8m^2\frac{(1-\omega^2)^{3/2}}{\omega^2}+6m^4\frac{(1-\omega^2)^{5/2}}{\omega^4}\right]\times E(1-m^2). \tag{7}$$

Despite the competing second- and fourth-order terms in Eq. (7), it can easily be seen that the interaction is *attractive*. Note that this is in agreement with our expectations, since soft nonlinearities should give the same type of interaction as NLS, where as noted above, the same parity pulse interaction is attractive [11].

Next, we elucidate the nature of the interaction as a function of the separation $L=2K(1-m^2)/c$ between the pulses of the lattice, as well as of the frequency $\omega$. However, from the above definition of $L$, we can express $m=m(L)$ and substitute into Eq. (7), to express the interaction term $V=E-E_{SB}$ (where $E_{SB}=16\sqrt{1-\omega^2}$, is the energy of a single breather), as a function of $(L,\omega)$. In Fig. 2, we show a plot of $V=V(L,\omega)$ as a function of its arguments. Furthermore, two-dimensional ''sections'' have been used for showing the dependence of $V=V(L,\omega=\text{fixed})$ and $V=V(L=\text{fixed},\omega)$. From the latter graphs also plotted in semilog and log-log scales, respectively, we clearly conclude that the dependence on $L$ is exponential, while the one on $\omega$ follows a power law. The deviation of the latter from a ''pure'' power-law dependence close to $\omega=1$ is because then the $1-\omega^2$ term is non-negligible and, hence, the dependence is more complicated, but still explicitly tractable through the analytical results given above.

In the case of NLS and its discrete version (DNLS), it can be shown that configurations containing structures of the same parity have as many unstable eigenvalues as the number of times the relative phase between neighboring pulses remains unchanged [11,12]. Hence, it is expected that breather lattice configurations should be unstable. We have verified this conjecture by means of direct numerical simulations. In the simulation of the problem, an eighth-order Runge-Kutta scheme was implemented [13]. Periodic boundary conditions were used and the initial condition contained an exact breather lattice configuration, matching the periodicity of the finite domain. Hence, the only perturbation to the problem came from the numerical discretization of the problem. We thus find, as can be seen in Fig. 3, that such a perturbation will grow and eventually destroy the breather lattice configuration. Similar results were found for all of the studied cases and parameter changes. We, thus, conclude that the breather lattice is unstable.

It should be noted that, as per the nature of the available *exact* solution of Eq. (1), only breathers oscillating in phase (and, thus, attracting each other) have been considered here. We are not aware of exact solutions of the continuum problem in which the breathers oscillate out of phase (and, thus, repel each other). In the discrete setting, however, one naturally expects such solutions to arise, as they do for the DNLS [11]. In the discrete case, it is expected that out-of-phase breather configurations *can* be linearly stable (for sufficiently discrete lattices), as they have been found to be in the case of DNLS in [11,14].

Another important question that naturally arises is how the picture presented here will be modified in approaching the anticontinuum limit (of lattices with lattice spacing $\to\infty$). In that case, the presence of the instability for in-phase pulse oscillations will not be affected, as the Floquet multipliers corresponding to the so-called ''interaction eigen-

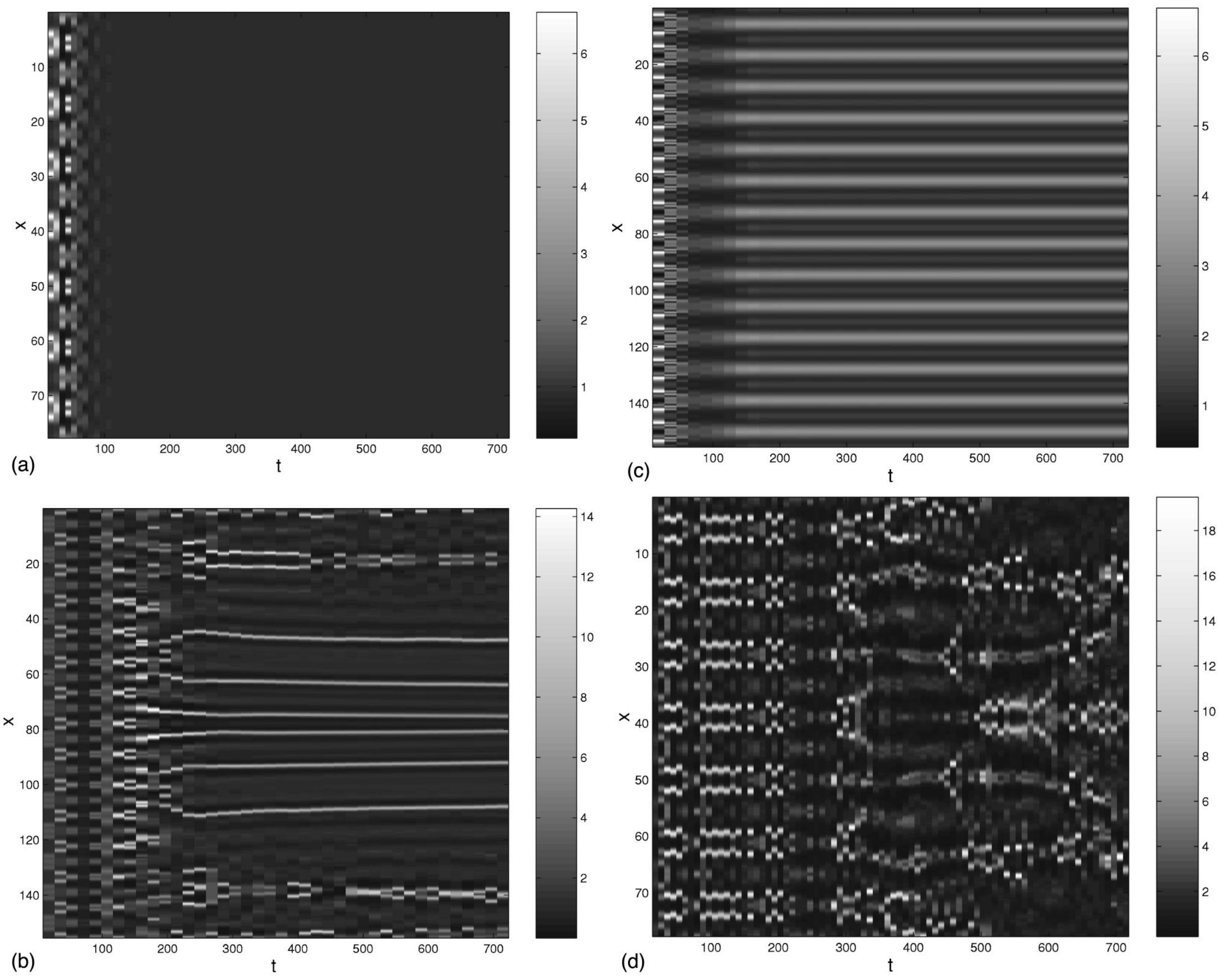


FIG. 4. The ac-driven and damped case: once again, space-time contour plots of the energy density are given. Panels (a) and (b) are both for $F_0=0.225$. In the top left panel, the initial condition contains 7 breathers in the lattice, while in the second one it contains 14. Panel (c) of the stabilized locked breather lattice occurs for $F_0=0.425$, while the intermittent pattern of panel (d) occurs for $F_0=0.310$ (also see text).

values'' of [11], will always be present and will be unstable. However, their specific value will depend on the lattice spacing. Hence, if the lattice spacing increases and so does the associated pulse separation, the instability will become weaker (i.e., the growth rate will decrease) and the time necessary for it to manifest itself, which is inversely proportional to the growth rate, will increase. In the case of discrete breathers oscillating out of phase, configurations close to the anticontinuum limit are expected to be linearly stable, as mentioned above. Nevertheless, as the continuum limit is approached, more ''exotic'' routes to instability, such as the Hamiltonian Hopf bifurcations [15] observed in the corresponding DNLS configurations (see, e.g., [16]), can be expected.

However, the question arises, whether stabilization of the breather lattice can be achieved in driven and damped situations studied previously in the dc case [17], and also for ac driving and small domains in [18]. The SG equation then becomes

$$u_{tt}=u_{xx}-\sin u+F_0 \sin(\omega t)-\alpha u_t, \tag{8}$$

where $\alpha$, the dissipation coefficient was fixed to 0.1 (the results were also checked to be representative for different values of $\alpha$) and $F_0$ was varied. $\omega$ was chosen to be the frequency of the breather lattice. The scenarios observed were, basically, similar to the ones reported in [18]. For small $F_0$ ($F_0<0.198$), the lattice smoothed out to a uniform spatial state (similar to the one observed in the top left panel of Fig. 4, but for a slightly higher value of $F_0=0.225$) and the response became identical to the periodic motion of the single pendulum (see [18], and references therein). For large $F_0$ ($F_0>0.427$), the response became highly irregular leading to chaotic dynamics. In the intermediate regime, however, suppression of chaotic behavior was observed by the generation and localization or intermittent behavior of pulse-like coherent structures. We do not attempt to give parameter regimes for the individual types of intermediate behavior since, as the first two (left-most) panels of Fig. 4 indicate, the corresponding parameter windows were relatively sensitive to initial conditions (i.e., these two panels show that the behavior was different for the same parameter values but different number of breathers in the initial condition). Instead, we summarize the main features of this regime:

(1) Regimes of locking to a breather lattice [such as $0.421 < F_0 < 0.427$; see panel (c) of Fig. 4]; it was also tested that such localization occurred independently of the number of breathers in the initial condition;

(2) Regimes of strongly intermittent behavior [see the panel (d) of Fig. 4] where the re-emergence of coherent excitations suppressed the appearance of chaos;

(3) Regimes of coexistence between the above situations (i.e., where a few breathers were strongly localized continuously while others were occasionally being regenerated), as well as parameter windows of uniform behavior and chaotic behavior. An important result, however, of these investigations is that *it is possible to lock the configuration either completely, or even partially (with respect to the initial condition), depending on the parameter values, into a breather lattice state, through driving and damping*.

Finally, we investigated two different limits of Eq. (1), suggested in [2]. For $k,m \rightarrow 1$ the limit gives the "pseudosphere" solution $u = 4\tan^{-1}(\tanh t/2)$, which resembles a $\pi$-kink, but in time rather than space [2]. The energy in this limit is

$$E = 4\pi - \frac{\pi}{2}(k-1)^2 + \frac{\pi}{4}(m-1)^2 + \frac{3\pi}{32}(m-1)^2(k-1)^2. \tag{9}$$

Note that $4\pi$ is the energy of a single pseudosphere, while the remaining terms yield the interaction energy $V = V(k,m)$. On the other hand, the $k \rightarrow$ finite, $m \rightarrow 0$ limit gives the kink-antikink pair solution $4\tan^{-1}(t\,\mathrm{sech}\,x)$. The energy in this case is given by

$$E = \left[16 - 8\left(k + \frac{1}{k}\right) + 2m^2\left(2 + 3k^2 + \frac{3}{k^2}\right)\right]E(1-m^2). \tag{10}$$

Once again, as expected from the physical intuition of the problem, the interaction is attractive in this limit.

In conclusion, using the exact breather lattice solution of the sine-Gordon equation we (i) obtained an attractive interaction between two breathers as a function of breather separation and frequency in the asymptotic limit, (ii) recovered the interaction energy between two pseudosphere solutions and a kink-antikink pair in the appropriate limits, (iii) numerically found the lattice solution to be unstable, and (iv) numerically demonstrated stabilization of the lattice through ac driving with damping. Our results should also be relevant for NLS and other breather-bearing nonlinear equations. An extension of our analysis and numerical results for the $2+1$ dimensional sine-Gordon equation would be highly desirable.

This research is supported by the U.S. Department of Energy, under Contract No. W-7405-ENG-36.

[1] R. K. Dodd, J. C. Eilbeck, J. D. Gibbon, and H. C. Morris, *Solitons and Nonlinear Wave Equations* (Academic Press, London, 1982).
[2] R. McLachlan, Math. Intelligencer **16**, 31 (1994).
[3] M. J. Ablowitz, D. J. Kaup, A. C. Newell, and H. Segur, Phys. Rev. Lett. **30**, 191 (1973); M. J. Ablowitz and H. Segur, *Solitons and the Inverse Scattering Transform* (SIAM, Philadelphia, 1981).
[4] J. D. Kress, A. Saxena, A. R. Bishop, and R. L. Martin, Phys. Rev. B **58**, 6161 (1998).
[5] A. Saxena, Y. S. Kivshar, and A. R. Bishop, Synth. Met. **116**, 45 (2001).
[6] D. Hennig, Phys. Rev. E **62**, 2846 (2000).
[7] J. Rubinstein, J. Math. Phys. **11**, 258 (1970).
[8] R. Dandoloff, S. Villain-Guillot, A. Saxena, and A. R. Bishop, Phys. Rev. Lett. **74**, 813 (1995).
[9] F. Fillaux, C. J. Carlile, and G. J. Kearley, Phys. Rev. B **58**, 11 416 (1998).
[10] T. Arai and M. Tajiri, Phys. Lett. A **274**, 18 (2000).
[11] T. Kapitula, P. G. Kevrekidis, and B. A. Malomed, Phys. Rev. E **63**, 036 604 (2001).
[12] B. Sandstede, Trans. Am. Math. Soc. **350**, 429 (1998).
[13] E. Hairer, S. P. Nørsett, and G. Wanner, *Solving Ordinary Differential Equations I: Nonstiff Problems* (Springer-Verlag, Berlin 1993).
[14] P. G. Kevrekidis, Phys. Rev. E (to be published).
[15] J.-C. van der Meer, Nonlinearity **3**, 1041 (1990).
[16] P. G. Kevrekidis, A. R. Bishop, and K. Ø. Rasmussen, Phys. Rev. E **63**, 036 603 (2001).
[17] J. C. Ariyasu and A. R. Bishop, Phys. Rev. B **35**, 3207 (1987); **39**, 6409 (1989).
[18] A. R. Bishop, K. Fesser, P. S. Lomdahl, W. C. Kerr, M. B. Williams, and S. E. Trullinger, Phys. Rev. Lett. **50**, 1095 (1983).